

## Novel 3,4-Isoxazolediamides as Potent Inhibitors of Chaperone Heat Shock Protein 90<sup>†</sup>

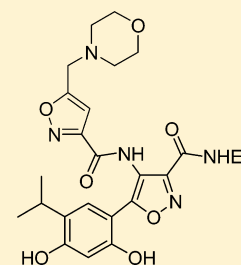
Riccardo Baruchello,<sup>‡</sup> Daniele Simoni,<sup>\*,‡</sup> Giuseppina Grisolia,<sup>‡</sup> Giuseppina Barbato,<sup>‡</sup> Paolo Marchetti,<sup>‡</sup> Riccardo Rondanin,<sup>‡</sup> Stefania Mangiola,<sup>‡</sup> Giuseppe Giannini,<sup>\*,§</sup> Tiziana Brunetti,<sup>§</sup> Domenico Alloatti,<sup>§</sup> Grazia Gallo,<sup>§</sup> Andrea Ciacci,<sup>§</sup> Loredana Vesci,<sup>§</sup> Massimo Castorina,<sup>§</sup> Ferdinando M. Milazzo,<sup>§</sup> Maria L. Cervoni,<sup>§</sup> Mario B. Guglielmi,<sup>§</sup> Marcella Barbarino,<sup>§</sup> Rosanna Foderà,<sup>§</sup> Claudio Pisano,<sup>§</sup> and Walter Cabri<sup>§</sup>

<sup>‡</sup>Dipartimento di Scienze Farmaceutiche, Università degli Studi di Ferrara, I-44121 Ferrara, Italy

<sup>§</sup>R&D Sigma-Tau Industrie Farmaceutiche Riunite S.p.A., I-00040 Pomezia, Roma, Italy

### Supporting Information

**ABSTRACT:** A structural investigation on the isoxazole scaffold led to the discovery of 3,4-isoxazolediamide compounds endowed with potent Hsp90 inhibitory properties. We have found that compounds possessing a nitrogen atom directly attached to the C-4 heterocycle ring possess in vitro Hsp90 inhibitory properties at least comparable to those of the structurally related 4,5-diarylisoxazole derivatives. A group of compounds from this series of diamides combine potent binding affinity and cell growth inhibitory activity in both series of alkyl- and aryl- or heteroarylamides, with IC<sub>50</sub> in the low nanomolar range. The 3,4-isoxazolediamides were also very effective in causing dramatic depletion of the examined client proteins and, as expected for the Hsp90 inhibitors, always induced a very strong increase in the expression levels of the chaperone Hsp70. In vivo studies against human epidermoid carcinoma A431 showed an antitumor effect of morpholine derivative **73** comparable to that induced by the reference compound **10**.



### INTRODUCTION

Heat shock proteins (Hsp's) play a key role in cell protection against various cell stress factors (e.g., toxic xenobiotic, chemotherapy, radiation), acting as a protective factor against the misfolding of essential proteins involved in maintaining cell functionality. Hsp90 proteins, members of these molecular chaperones, are proteins that play a key role in the conformational maturation, stability, and function of so-called "client" proteins.<sup>1–3</sup> The inhibition of Hsp90 triggers the disruption of the Hsp90–client protein complex, and subsequently its proteasome-mediated degradation causes loss of function and inhibition of cell growth. Many Hsp90 client proteins are overexpressed in cancer, often in mutated forms, and are responsible for unrestricted cancer cell proliferation and survival. Interestingly, heat shock protein 90 has emerged as an important target in several diseases.<sup>4–9</sup> In particular, the role played by Hsp90 in regulating and maintaining the transformed phenotype in cancers and neurodegenerative diseases has been recently identified, as well as its roles in fungal and viral infections.<sup>10–12</sup>

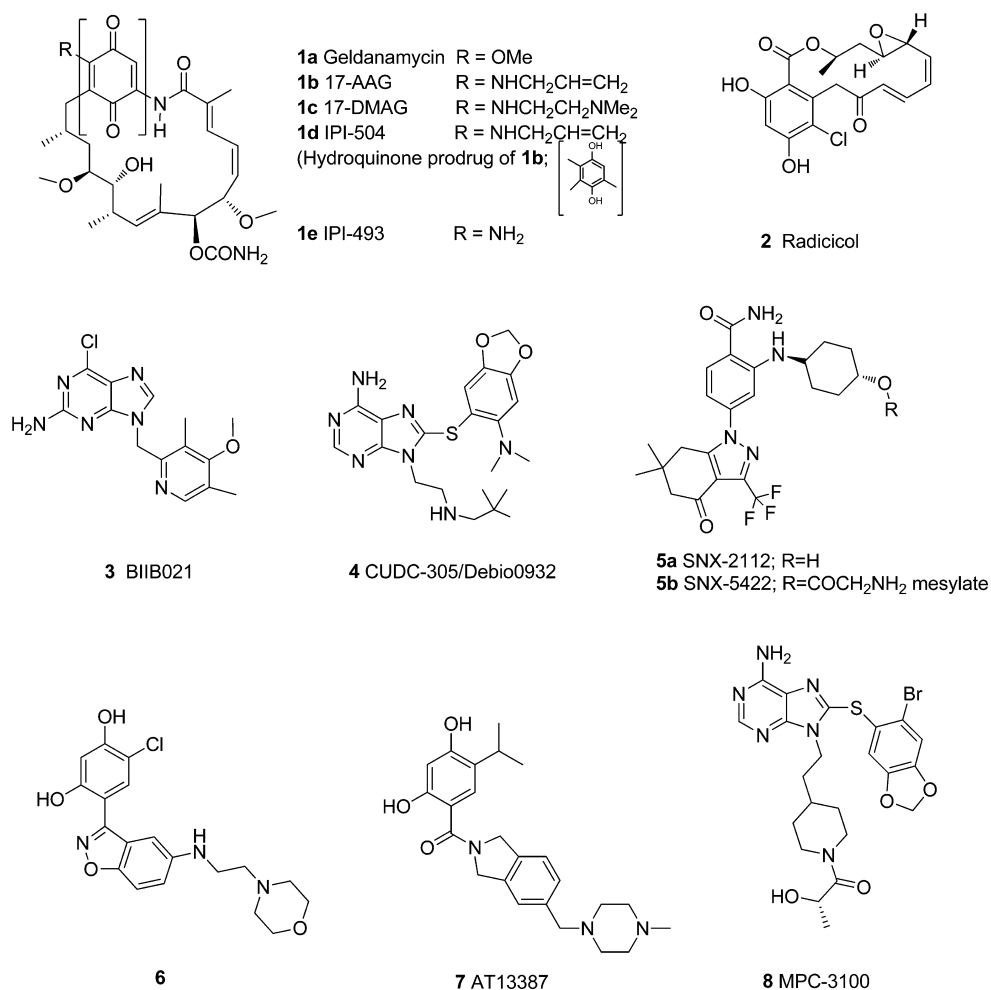
Inhibition of the ATPase activity of Hsp90 disrupts an ongoing "folding" cycle, involving multiple cochaperone proteins, and in turn leads to destabilization, ubiquitination, and ultimately proteasomal degradation of client proteins.<sup>13–15</sup> Hsp90 is normally expressed in normal cells, representing 1–2% of the total intracellular protein, from which about 3% is found in the nucleus with effects on the regulation of several nuclear events.<sup>16</sup> Under stress conditions, such as in tumors, its levels increase to 4–6% of the whole proteomic load of the cell.<sup>17–19</sup>

Hsp90 derived from tumor cells has particularly high ATPase activity with higher binding affinity to Hsp90 inhibitors than the latent form in normal cells, allowing selective targeting of Hsp90 inhibitors to tumor cells with little inhibition of Hsp90 function in normal cells.<sup>9</sup> In addition, Hsp90 has also been recently identified as an important extracellular mediator for tumor invasion.<sup>20–22</sup> Thus, Hsp90 is considered a major therapeutic target for anticancer drug development because inhibition of a single target represents attack on all of the hallmark traits of cancer. Since the discovery that two natural compounds, geldanamycin (**1a**) and radicicol (**2**) (Figure 1), were able to inhibit Hsp90 function through binding to the ATP binding pocket in its N-terminal domain, the interest for Hsp90 inhibitors has grown. The natural antibiotic geldanamycin was shown to exhibit potent antitumor activity against human cancer cells,<sup>23</sup> but significant toxicities prevented its clinical development.<sup>24</sup>

The first-in-class Hsp90 inhibitor to enter clinical trials was the geldanamycin analogue 17-allylaminogeldanamycin (17-AAG, **1b**, Figure 1). Even though high in vitro activity characterizes this geldanamycin derivative, its interest is shadowed by poor solubility coupled to hepatotoxicity properties. Some of these problems have been partially solved by the discovery of 17-dimethylaminoethylamino-17-demethoxygeldanamycin (17-DMAG, **1c**, Figure 1). Infinity is developing two drug

Received: August 30, 2011

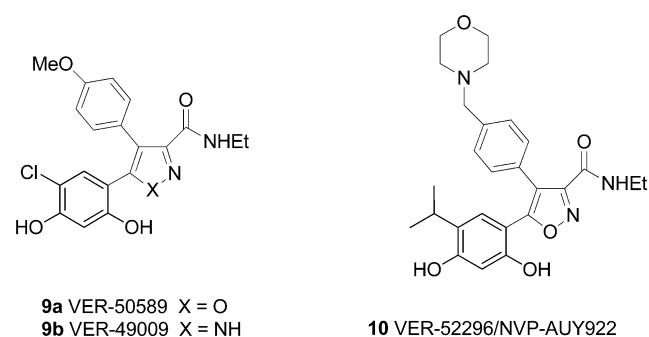
Published: November 9, 2011



**Figure 1.** Hsp90 inhibitors: natural compounds and some drugs currently in clinical trials.

candidates in its Hsp90 chaperone inhibitor program: retaspimycin hydrochloride (IPI-504, **1d**, Figure 1), an intravenously administered small molecule, and IPI-493 (**1e**, Figure 1), which is administered orally.<sup>25</sup> Radicicol (**2**, Figure 1), a natural macrocyclic antifungal antibiotic, was found to inhibit Hsp90 protein by interacting at the same site of action of geldanamycin.<sup>26</sup> However, because of its intrinsic chemical instability, it is deprived of in vivo activity. After pioneering studies with natural products geldanamycin and radicicol, many selective Hsp90 inhibitors from various institutions have been disclosed and entered into clinical trials.<sup>27,28</sup> The purine scaffold is another important class of Hsp90 inhibitors.<sup>29,30</sup> This class of derivatives was devised by structural homology with ATP. Among the many inhibitors developed within this family, BIIB021 (**3**), investigated by Chiosis and co-workers,<sup>30</sup> and CUDC-305 (**4**), developed by Curis Inc. (Figure 1), have entered into clinical trials.<sup>31</sup> The *o*-aminobenzoic acid derivative SNX-2112 (**5a**) and its prodrug SNX-5422 (PF-04929113) (**5b**) (Figure 1), proposed by Serenex Inc., are also under clinical investigation.<sup>32</sup> High-throughput screening campaigns permitted the discovery of benzoisoxazole derivative **6**, having a resorcinol moiety in position 3, that has also been disclosed as a potent Hsp90 inhibitor.<sup>33</sup> Other resorcinols, AT13387 (**7**) by Astex and ganetespib by Synta Pharmaceuticals Corp. (chemical structure not yet disclosed), entered recently into clinical trials.<sup>34–36</sup>

Myrexis has reported MPC-3100 (**8**) (Figure 1), an orally bioavailable small-molecule Hsp90 inhibitor, as well as its more water-soluble prodrug MPC-0767.<sup>37,38</sup> Among the different classes of Hsp90 inhibitors, researchers from Vernalis Ltd. and Institute of Cancer Research (U.K.) have disclosed the 4,5-diarylpyrazoles,<sup>39</sup> 3-aryl-4-carboxamide pyrazoles,<sup>40</sup> 4,5-diaryl-isoxazoles,<sup>41</sup> 3,4-diarylpyrazole derivatives,<sup>42,43</sup> and thieno[2,3-*d*]pyrimidines.<sup>39,42,44,45</sup> Investigations on 4,5-diaryl-isoxazoles **9a** (VER-50589, Figure 2) generated Hsp90 inhibitors that proved

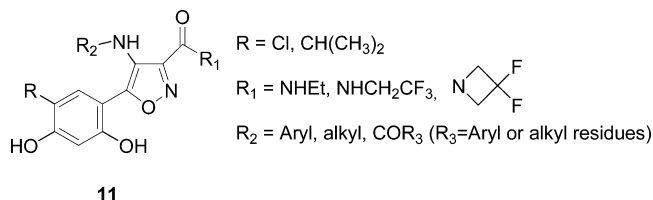


**Figure 2.** Hsp90 inhibitors with a 4,5-diaryl-isoxazole/pyrazole scaffold.

to be from 5 to 50 times more active at inhibiting cancer cell proliferation compared to the previously reported 4,5-diarylpyrazoles **9b** (VER-49009, Figure 2). Thus, the 4,5-diaryl-isoxazole

scaffold bearing a resorcinol at position 5 was considered a prerequisite for the activity on Hsp90, and compound **10** (VER-52296/NVP-AUY922, Figure 2), currently in phase II clinical trials, belongs to this class of compounds. However, to date, no Hsp90 inhibitors in clinical trials fully satisfy the requisites of safety and stability. Some of the drugs under clinical investigation have showed toxicity toward liver, eyes, stomach–intestine, and heart.<sup>35,46</sup> Therefore, the need for potent and selective Hsp90 inhibitors still remains an interesting and promising goal.

In continuation of our antitumor drug-discovery project<sup>47</sup> we have recently undertaken a detailed structural investigation on a new class of 3,4-isoxazolidiamides **11** (Figure 3). We mainly



**Figure 3.** General structure of new Hsp90 inhibitors used in these study.

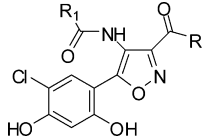
focused our attention on the C-4 position of the isoxazole scaffold where we found that compounds possessing a nitrogen atom directly attached to the heterocycle ring possess in vitro Hsp90 inhibitory properties comparable to those of the structurally related 4,5-diarylisoxazoles. Herein, we will give full details on the synthesis and pharmacological characterization of a new class 3,4-isoxazolidiamides as potent Hsp90 inhibitors. A group of compounds that combine notable binding properties and potent cell growth inhibitory activity will be described. Additionally, the in vivo activity of the 3,4-isoxazolidiamides **49** and **73** against human epidermoid carcinoma A431 will be also reported.

## CHEMISTRY

The synthetic route used for the preparation of amides **15–73** (see Tables 1, 3, and 4) is shown in Scheme 1. The 4-nitroisoxazoles **13a–d** were synthesized by chemoselective nitration of the isoxazoles **12a–d**<sup>41</sup> using concentrated nitric acid and acetic anhydride. Compounds **12b,c** were prepared starting from the appropriate ester derivative with the following sequence of reactions (as in Supporting Information): (a) hydrolysis of ester moiety, (b) activation of resulting carboxylic acid, and (c) subsequent reaction with the proper commercially amines. Reduction of the nitro compounds **13a–d** to give **14a–d** in good yields was done using zinc powder and ammonium chloride in a mixture of water and tetrahydrofuran as solvents. Reaction of the amines **14a–d** with the proper commercially available acyl chloride gave the corresponding dibenzylated amides that after deprotection of phenolic groups with boron trichloride furnished the desired amides **15–73**.

The morpholine derivatives **77a–e** and **79a,b** and the piperazine derivative **79c** were synthesized as reported in Scheme 2. The alcohols **74a–e** were simply prepared starting from the amine **14d** by reaction with the adequate acyl chloride. The alcohols **74a–e** were then activated as the corresponding mesylate derivatives by reaction with mesyl chloride in methylene chloride prior to being reacted with morpholine to give **76a–e**. Removal of benzylic protecting groups using boron trichloride furnished the final **77a–e**

**Table 1.** Data for Isoxazole-3,4-diamides: Binding on Hsp90 by a Fluorescence Polarization Assay (FP Assay) and Cytotoxicity on NCI-H460 Non-Small-Cell Lung Carcinoma Cells



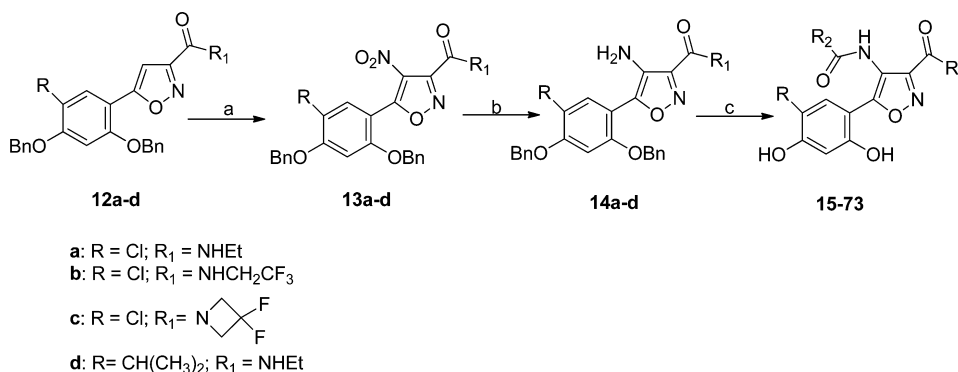
Compound	R	R <sub>1</sub>	NCI-H460 (IC <sub>50</sub> ; μM)	Hsp90 (FP) (IC <sub>50</sub> ; μM)
<b>10</b>	-	-	0.0024	0.061
<b>15</b>	CH <sub>3</sub> CH <sub>2</sub> -NH-		> 1	0.153
<b>16</b>	CH <sub>3</sub> CH <sub>2</sub> -NH-		> 1	0.184
<b>17</b>	CH <sub>3</sub> CH <sub>2</sub> -NH-		> 1	0.163
<b>18</b>	CH <sub>3</sub> CH <sub>2</sub> -NH-		> 1	0.130
<b>19</b>	CH <sub>3</sub> CH <sub>2</sub> -NH-		0.410	0.074
<b>20</b>	CH <sub>3</sub> CH <sub>2</sub> -NH-		> 1	0.037
<b>21</b>	CH <sub>3</sub> CH <sub>2</sub> -NH-		0.31	0.085
<b>22</b>	CH <sub>3</sub> CH <sub>2</sub> -NH-		> 1	0.167
<b>23</b>	CH <sub>3</sub> CH <sub>2</sub> -NH-		0.750	0.250
<b>24</b>	CF <sub>3</sub> CH <sub>2</sub> -NH-		> 1	0.160
<b>25</b>			> 1	> 100
<b>79a</b>	CH <sub>3</sub> CH <sub>2</sub> -NH-		0.130	0.168

in good yields. Similarly, removal of benzylic groups from **74a–e** gave the deprotected derivatives **75a–e**. The derivatives **78a–c** were obtained by reaction of **14a,d** with acryloyl chloride, and the resulting acryloyl amides were then reacted through a Michael addition reaction with morpholine or 1-methylpiperazine. Removal of the benzylic protecting groups by means of boron trichloride yielded the desired compounds **79a–c**.

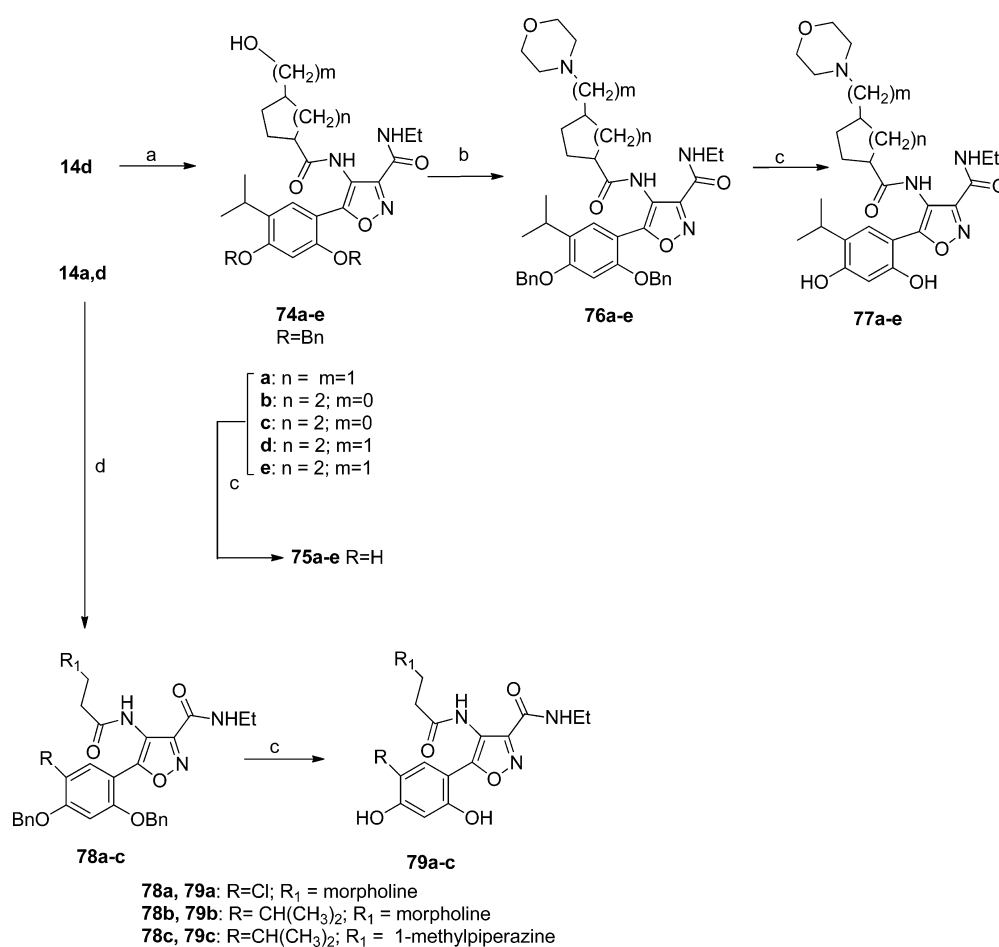
The synthesis of amines **81a–d** is described in Scheme 3. The amine **14a** was first debenzylated using boron trichloride. The reductive amination reaction of the resulting resorcinol derivative **80** by means of sodium cyanoborohydride and a proper aldehyde or ketone furnished the desired amines **81a–d** in moderate to good yields.

## RESULTS AND DISCUSSION

In our project, we systematically investigated possible modifications on the isoxazole scaffold, focusing mainly our

Scheme 1<sup>a</sup>

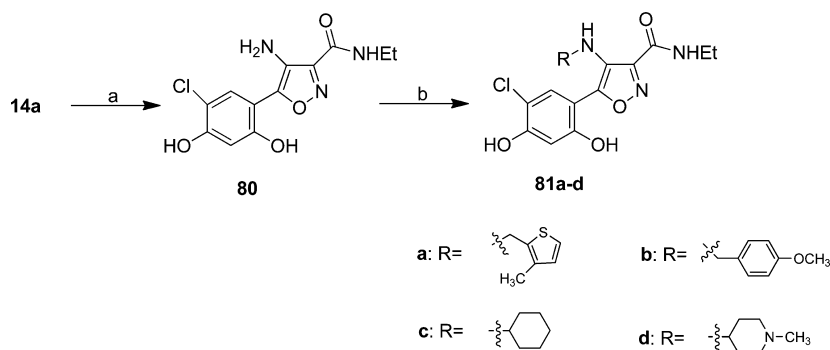
<sup>a</sup>Reagents and conditions: (a) conc HNO<sub>3</sub>/Ac<sub>2</sub>O; (b) Zn, H<sub>2</sub>O/THF, NH<sub>4</sub>Cl; (c) (i) R<sub>2</sub>COCl, TEA, DCM; (ii) BCl<sub>3</sub>, DCM, 0 °C.

Scheme 2<sup>a</sup>

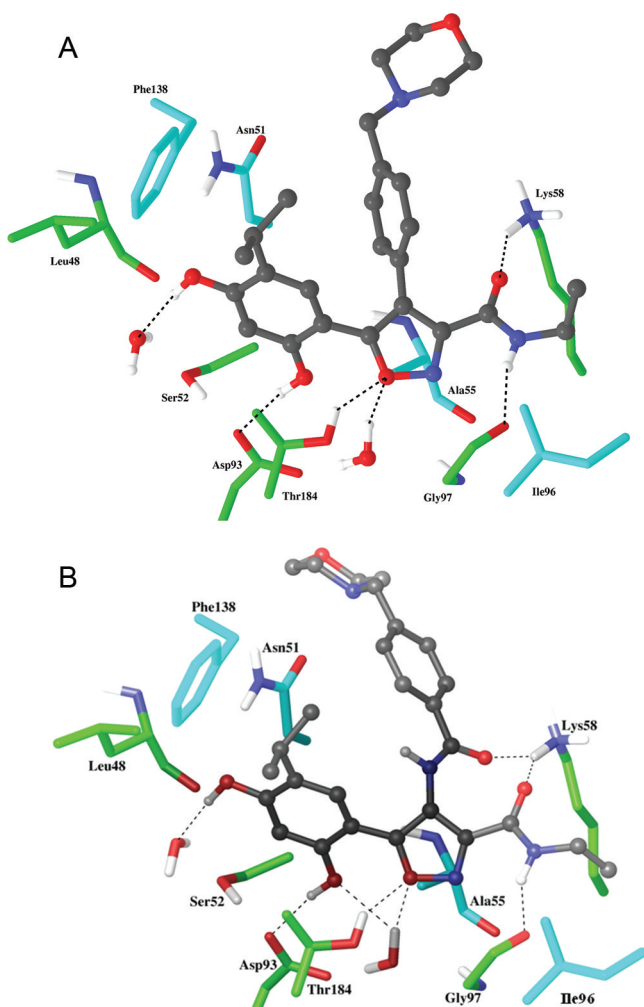
<sup>a</sup>Reagents and conditions: (a) (i) acyl chloride, TEA, DCM; (ii) BF<sub>3</sub>·Et<sub>2</sub>O, DCM, 0 °C; (b) (i) mesyl chloride, DIPEA, DCM; (ii) morpholine, 70 °C; (c) BCl<sub>3</sub>, DCM, 0 °C; (d) (i) acryloyl chloride, TEA, DCM; (ii) morpholine or 1-methylpiperazine, reflux.

attention on the C-4 position. As reported above, among the structural classes of compounds that have provided interesting results as potential Hsp90 inhibitors, the 4,5-diarylisoxazoles are of remarkable importance having recently led to **10** (VER-52296/NVP-AUY922, Figure 2) currently in phase II clinical trials.<sup>27</sup> Crystal structures of Hsp90 N-terminal domain in complex with several inhibitors have been well described in literature: in Figure 4A the active site of Hsp90 cocrystallized with **10** (PDB code 2VCI) is reported.<sup>41</sup> A network of

hydrogen-bonding interactions involving the resorcinol moiety and the heterocyclic ring with Asp93, Thr184, and a cluster of structurally conserved and highly ordered water molecules characterize the key interactions of the compound with protein. A bulky hydrophobic group interacts with the lipophilic pocket created by Phe138, Met98, Val150, Leu103, Leu107, Trp162, and Tyr139; additional hydrogen bonding interactions involve the 3-amide group with Gly97 and Lys58. We hypothesized that the introduction of a second amide group at C-4, as shown

Scheme 3<sup>a</sup>

<sup>a</sup>Reagents and conditions: (a)  $\text{BCl}_3$ , DCM, 0 °C; (b) (i) appropriate aldehyde or ketone, MeOH, AcOH 0.1%; (ii)  $\text{NaCNBH}_3$ .



**Figure 4.** (A) VER-52296/NVP-AUY922 (compound **10**) cocrystallized in Hsp90 active site (PDB code 2VCI). Color scheme is by atom type: gray, VER-52296/NVP-AUY922; cyan, protein residues involved in nonpolar interactions; green, protein residues involved in polar interactions. H-Bonds are shown as dotted lines. (B) Docking pose of compound **49** in Hsp90 active site. Color scheme is by atom type: gray, **49**; cyan, protein residues involved in nonpolar interactions; green, protein residues involved in polar interactions. H-Bonds are shown as dotted lines.

for compound **49** (Figure 4B), could play an additional role in the interaction with the protein, producing an extra interaction with Lys58, as well as a concomitant reorientation of the

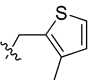
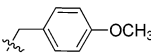
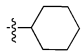
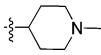
aromatic portion. The key interactions of the OH-resorcinol groups and the C-3 amide still remain identical. Thus, the idea of an additional H-bond donor interaction in the active site, mediated by an amide moiety at position 4 of the isoxazole ring, was considered as the basic structural motif for the construction of a series of 3,4-isoxazolidiamides<sup>48</sup> as those reported in Tables 1, 3, and 4. The resorcinol portion and the C-3 amide moiety were maintained unaltered considering the privileged role offered by these fragments in the interaction with the Hsp90 protein in both radicicol and 4,5-diarylisoxazole series of compounds.<sup>41</sup>

The feasibility of the project was first investigated by preparing a small explorative series of compounds bearing a 5-chlororesorcinol residue at the C-5 position. Meanwhile the amides at C-3 and C-4 of the isoxazole ring were varied as shown in Table 1. The 5-chloro substitution was at the beginning chosen for ease of synthesis; moreover, 5-unsubstituted resorcinols are known to be less active with respect to the substituted ones.<sup>42</sup>

All the synthesized compounds were tested for their potential Hsp90 inhibitory properties. Measurements of binding were by a fluorescence polarization (FP) assay, and inhibition of cell growth proliferation of the NCI-H460 tumor cell line was determined.

It was apparent from the results shown in Table 1 that the strategy of the C-4 amide moiety could lead to compounds useful as Hsp90 inhibitors. All the synthesized compounds, apart from the fluorinated derivative **25**, showed binding affinity in the range of 37–250 nM. Compounds **19**, **21**, **23**, and **79a** also showed cytotoxic activity in the submicromolar range (130–750 nM). The fluorinated compound **24**, synthesized to further reinforce the H-bond with Lys58, contrary to our expectation, showed equivalent binding and cellular activity, thus demonstrating no advantage compared with the related ethylamide residue **16**. The other fluorinated derivative **25**, where the hydrogen on the C-3 amide was missing, was inactive, reinforcing the importance of the presence of a hydrogen in this position for its H-bond capabilities and minimal steric hindrance. The C-4-aminoalkyl derivatives **81a–d** (Table 2) were synthesized and screened to better substantiate our structure–activity investigation. Amine compounds **81a,b** (Table 2) showed a drop in binding affinity when compared with the parent amides **19** and **16**. Furthermore, the observed drop with regard to affinity was corroborated by the absence of cytotoxicity. A loss of a putative interaction of C-4 amide carbonyl with Lys58 as shown in the Figure S1 of compound **81b** could explain in some way the

**Table 2.** Data for the 4-Aminoisoxazoles: Binding on Hsp90 (FP Assay) and Cytotoxicity on NCI-H460 Non-Small-Cell Lung Carcinoma Cells

Compound	R	NCI-H460 (IC <sub>50</sub> ; μM)	Hsp90 (FP) (IC <sub>50</sub> ; μM)
<b>10</b>	-	0.0024	0.061
<b>81a</b>		> 1	0.230
<b>81b</b>		> 1	0.430
<b>81c</b>		> 1	0.620
<b>81d</b>		> 1	1.600

decrease of binding affinity. Anyway, the loss of cytotoxic activity shown by all the C-4 amines **81a–d** allowed us to view this type of substitution with little interest.

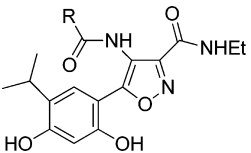
The interesting activity shown by some chlororesorcinol diamides gave confirmation of the idea that manipulation around the C-4 region of the isoxazole scaffold may significantly alter the binding of the compounds, providing an interesting opportunity for the construction of novel series of Hsp90 inhibitors. We further explored the potential of the new scaffold, investigating a series of additional substitutions at the C-4 amide portion. Given that substitution of the chlorine atom on the resorcinol moiety with an isopropyl group had proved to improve cytotoxicity,<sup>41</sup> isopropyl analogues have been synthesized. We carried out virtual docking experiments, using the Hsp90–**10** X-ray complex structure and a virtual library of 3,4-isoxazolidiamides bearing diverse C-4 substituents. Such a library was prepared by “reacting” the debenzylated intermediate **14d** with 350 commercially available acyl chlorides or carboxylic acids having molecular weights between 100 and 350. The resulting 3,4-isoxazolidiamides were filtered according to the rule of 5 < 2 (except **35–37** with two violations), subjected to a conformational analysis, and then docked in the active site of the enzyme. Compounds with scoring value higher than that of the simplest analogue (acetamide derivative **26**) were selected for synthesis. Scoring values for synthesized compounds are reported in Table S1. Biological evaluation of a library of 60 isopropyl derivatives (Tables 3 and 4) showed binding affinity in the range of 1–260 nM. Several compounds combined notable binding properties with potent cell growth inhibitory activity, i.e., IC<sub>50</sub> values in the low nanomolar range: **26**, **27**, **31**, **43** (Table 3) in the class of alkyl and cycloalkyl derivatives; **46**, **47**, **49** in the class of phenyl derivatives; **55–58**, **68**, **71**, and **72** in the class of heterocyclic derivatives (Table 4). The antiproliferative effects of compounds **28** and **30** were also noteworthy (16 and 42 nM, respectively) notwithstanding a decrease of their binding activity.

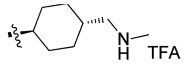
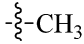
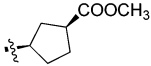

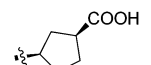
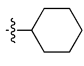
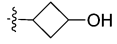
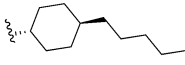
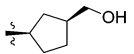
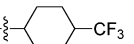
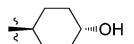
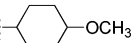
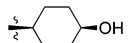
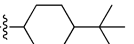
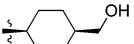
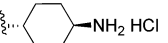
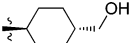
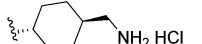
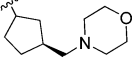
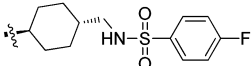
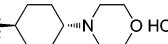
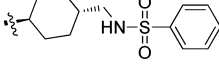
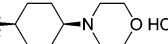
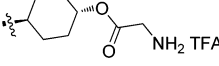
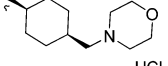
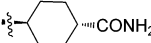
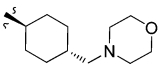
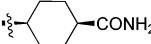
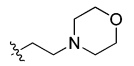
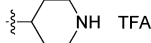
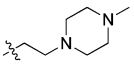
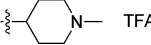
Interestingly, the morpholine water solubilizing group in compounds **49**, **73**, **77a,d,e** and **79b** was well tolerated as demonstrated by the binding and cell growth inhibiting properties of such compounds. Unfortunately, a group of compounds (i.e., **32–42**, **44**, **45**, **48**, **50–54**, **60–63**, **65–67**, **69**, **70**, **73**, **75a–e**, and **77b,c**) despite possessing an excellent binding profile showed only poor cell proliferation inhibitory properties. Such behavior can be accountable to permeability issues across cell membranes. Indeed, some compounds presented a large polar surface (i.e., **35–39**, **44**, **54**, **60–62**, and **73**; Table S1) or positively charged appendages at pH 7.4 (i.e., **33**, **34**, **40**, and **41**) as demonstrated by the LogD<sup>7.4</sup> parameter disclosed in Table S1. Instead, a lipophilicity index of  $3.2 \pm 0.7$  (i.e., log *P* parameter in Table S1), calculated using ACD/Labs software, does correlate to a high cytotoxicity profile (i.e., **27**, **28**, **31**, **43**, **46**, **47**, **55**, **57**, and **58**).

To validate that the antiproliferative activity of these compounds was indeed related to the inhibition of Hsp90, a few selected compounds (**27**, **28**, **31**, **49**, **55**, and **57**) were further tested for their effects on the expression of some typical Hsp90 client proteins in the A431 (human epidermoid carcinoma) cell line. The examined client proteins (Akt, Cdk4, and EGFR) and Hsp70 were evaluated by means of the classical Western blotting analysis on total protein extracts of A431 cells, following a 24 h exposure to various concentrations of the test compounds. All tested compounds were very effective, causing dramatic depletion of the examined client proteins and, as expected for the Hsp90 inhibitors, always inducing a very strong increase in the expression levels of the chaperone Hsp70 (Figure 5 and Figures S2–S4). The depletion was always dose dependent and was achieved with potency similar to that of the reference compound (17-DMAG). The only partial exception was represented by compound **55**, which caused a marked depletion of EGFR and CDK4 client proteins but, at the same time, showed only a marginal effect on the expression of Hsp70. These results therefore support the premise that the effects on cell growth of the 3,4-isoxazolidiamides were a consequence of their Hsp90 chaperone inhibitory properties.

Finally, 12 compounds (see Tables 3 and 4) were selected for in vivo study against human epidermoid carcinoma A431 tumor xenografts (Table S3 show the results of cytotoxicity assay of the compounds tested in vivo on A431 cell lines). All compounds were administered intraperitoneally once daily at their maximum tolerated doses (i.e., doses that produced a body weight loss of 7–8%) without any sign of toxicity. Compound **73** showed an antitumor effect (tumor volume inhibition of 48%) comparable to that of the reference compound **10** (Table 5 and Figure 6).<sup>49</sup> In contrast, compound **49**, structurally related to the reference compound **10** (NVP-AUY922), showed a reduced in vivo activity. The ability of **73** to affect in vivo the expression of typical Hsp90 client proteins was assessed in A431 tumor xenografts 2 h after the last treatment. As shown in Figure 7, **73** induced a strong degradation of three typical “client” proteins (EGFR, Akt, and CDK-4) and significantly increased the expression levels of Hsp70, with a potency comparable to that of the reference inhibitor **10** (NVP-AUY922). Thus, although in vitro activity of **73** is somehow moderate, the compound still shows a very good in vivo activity profile among those tested.

**Table 3. Data for Isoxazole-4-alkyl- and Cycloalkylamides: Binding on Hsp90 (FP Assay) and Cytotoxicity on NCI-H460 Non-Small-Cell Lung Carcinoma Cells<sup>b</sup>**



Compound	R	NCI-H460 (IC <sub>50</sub> ; μM)	Hsp90 (FP) (IC <sub>50</sub> ; μM)	Compound	R	NCI-H460 (IC <sub>50</sub> ; μM)	Hsp90 (FP) (IC <sub>50</sub> ; μM)
10	-	0.0024	0.061	42		> 1	0.0086
26*		0.081	0.055	43*		0.022	< 0.005 <sup>a</sup>
27*		0.024	0.041	44		> 1	0.039
28*		0.016	0.190	45		0.920	0.014
29		> 1	0.260	75a		0.260	0.0126
30		0.042	0.240	75b		> 1	< 0.005 <sup>a</sup>
31*		0.013	0.024	75c		0.500	< 0.005 <sup>a</sup>
32		0.200	0.030	75d		0.870	0.015
33		> 1	0.028	75e		0.600	< 0.005 <sup>a</sup>
34		> 1	0.040	77a		0.170	0.012
35		0.640	0.0054	77b		0.680	< 0.005 <sup>a</sup>
36		> 1	< 0.005 <sup>a</sup>	77c		0.610	0.0074
37		> 1	< 0.005 <sup>a</sup>	77d		0.140	0.0196
38		> 1	< 0.005 <sup>a</sup>	77e		0.130	0.0088
39		0.990	< 0.005 <sup>a</sup>	79b		0.110	0.214
40		> 1	< 0.005 <sup>a</sup>	79c		> 1	0.120
41		> 1	0.024				

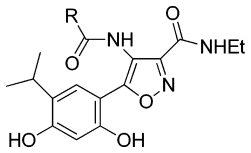
<sup>a</sup>For the detection limits of the assay, see Chiosis et al.<sup>50</sup> <sup>b</sup>The asterisk (\*) indicates that the compound was submitted to in vivo studies.

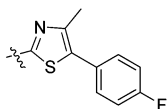
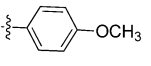
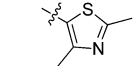
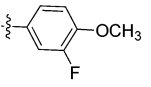
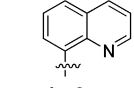
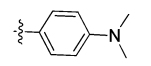
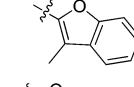
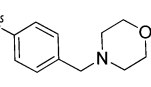
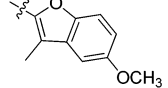
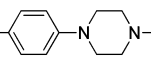
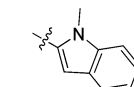
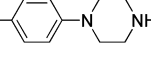
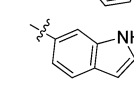
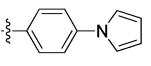
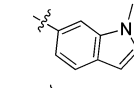
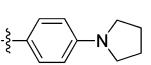
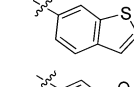
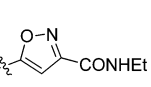
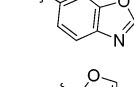
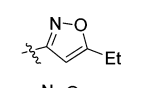
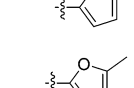
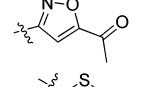
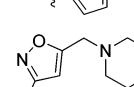
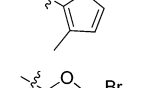

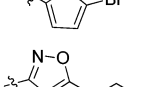
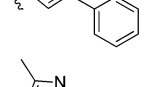
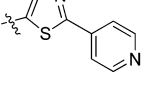
## CONCLUSION

We postulated that the introduction of a second amide group at the C-4 position of the 4,5-diarylisoxazoles scaffold could represent an interesting opportunity for the construction of a novel class of Hsp90 inhibitors. We have performed a detailed investigation and elaboration of the isoxazole scaffold, leading to the discovery of a novel class of 3,4-isoxazolidiamides

endowed with potent Hsp90 inhibitory activity. The C-4 amide appendage could be either an alkyl or aryl moiety. A group of amides showed affinity for the target comparable to that shown by 4,5-diaryl products **9a,b** and **10**. Compounds of interest that combine potent binding and cell growth activity were obtained in a series of alkyl- and cycloalkyldiamides (**26**, **27**, **31**, and **43**), as well as in a series of the aryl and heteroaryl derivatives

**Table 4.** Data for Isoxazole-4-aryl- and Heteroarylamides: Binding on Hsp90 (FP Assay) and Cytotoxicity on NCI-H460 Non-Small-Cell Lung Carcinoma Cells<sup>b</sup>



Compound	R	NCI-H460 (IC <sub>50</sub> ; μM)	Hsp90 (FP) (IC <sub>50</sub> ; μM)	Compound	R	NCI-H460 (IC <sub>50</sub> ; μM)	Hsp90 (FP) (IC <sub>50</sub> ; μM)
10	-	0.0024	0.061	61		> 1	0.040
46*		0.017	0.026	62		0.560	0.010
47		0.055	0.034	63		0.490	0.036
48		0.240	0.034	64		> 1	0.260
49*		0.095	0.071	65		0.750	0.048
50		> 1	0.024	66		0.360	0.062
51		> 1	0.032	67		0.170	0.033
52		> 1	0.032	68		0.087	0.034
53		0.810	0.022	69		0.180	0.020
54		> 1	0.024	70		0.110	0.015
55*		0.022	0.020	71*		0.022	< 0.005 <sup>a</sup>
56		0.082	0.019	72		0.016	< 0.005 <sup>a</sup>
57*		0.017	0.084	73*		0.200	0.040
58*		0.019	0.022				
59		> 1	0.250				
60		> 1	0.027				

<sup>a</sup>For the detection limits of the assay, see Chiosis et al.<sup>50</sup> <sup>b</sup>The asterisk (\*) indicates that the compound was submitted to in vivo studies.

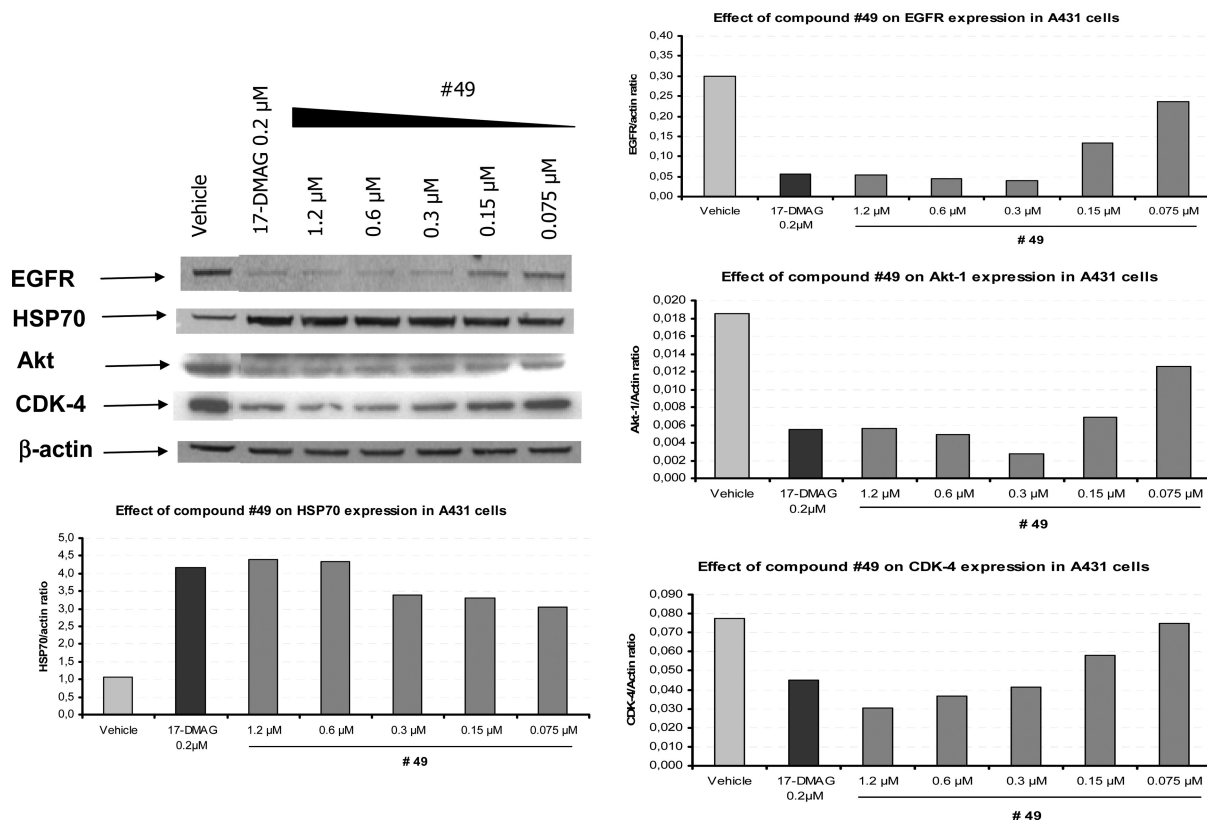
(46, 47, 49, 55–58, 68, 71, and 72). The antiproliferative effects of compounds 28 and 30 (16 and 42 nM, respectively) were notable notwithstanding the compounds having rather moderate binding affinities.

Analysis of the degradation of the client proteins in A431 cells proved that the antiproliferative effects of the diamides were indeed related to the inhibition of Hsp90. As expected for

Hsp90 inhibitors, the tested diamides induced a very strong increase in the expression levels of the chaperone Hsp70.

Twelve compounds with a different range of in vitro profile were selected to be studied in vivo against human epidermoid carcinoma A431. Compound 73 revealed an antitumor effect (tumor volume inhibition of 48%) comparable to that of the reference compound 10.

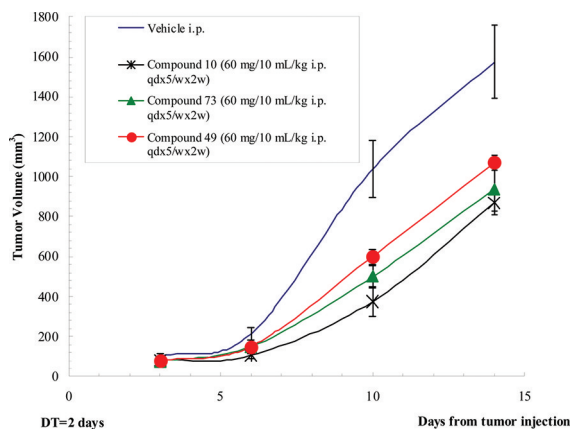




**Figure 5.** Analysis of Hsp90 client protein levels (EGFR, Akt, CDK-4) and Hsp70 in A431 tumor cells treated with compound 49. Total cellular extracts were obtained 24 h after treatment. Actin is shown as a control for protein loading. Results of densitometry analysis were reported as normalized (to  $\beta$ -actin) ratios.

**Table 5. Antitumor Activity of Compounds 49 and 73 in Comparison with 10 (NVP-AUY922) against A431 Epidermoid Carcinoma**

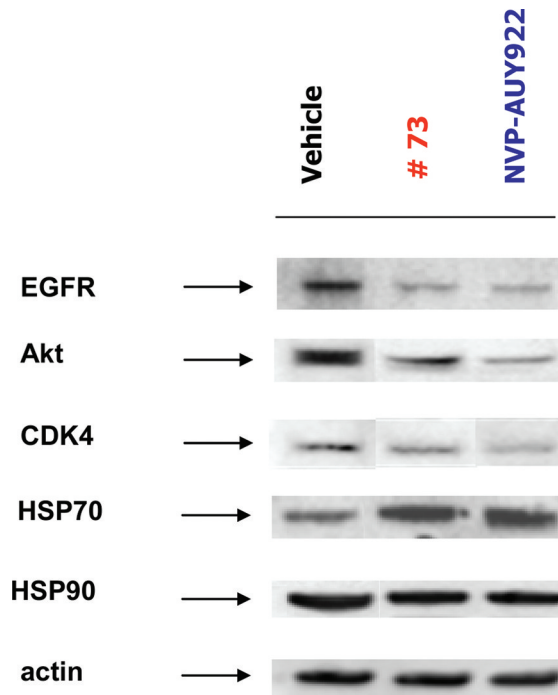
drug treatment	dose/route (mg/kg)	TVI $\pm$ SE (%)	BWL (%)
10	60/ip	48 $\pm$ 5	8
49	60/ip	33 $\pm$ 4	2
73	60/ip	48 $\pm$ 4	7



**Figure 6.** Antitumor activity of the compounds 49 and 73 in comparison with that of compound 10 (NVP-AUY922) against A431 epidermoid carcinoma xenografted in CD1 nude mice.

**EXPERIMENTAL SECTION**

**Tumor Xenograft Model.** Experiments were carried out at Sigma-Tau (Rome, Italy) using female athymic nude CD-1 mice,



**Figure 7.** Analysis of Hsp90 client protein levels (EGFR, Akt, CDK-4, and Hsp70) in A431 tumor xenografts, following treatment with 73 and 10 (NVP-AUY922). Total proteins were purified 2 h after the last treatment. Actin is shown as a control for protein loading. A representative blot is shown.

8–11 weeks old (Harlan, Italy). Mice were maintained in laminar flow rooms with constant temperature and humidity. Experimental

protocols were approved by the Ethic Committee for Animal Experimentation.

A431 epidermoid carcinoma cells ( $3 \times 10^6$ /mouse) were inoculated subcutaneously (sc) in the right flank of CD1 nude mice. Drug treatments started 3 days after tumor injection according to the schedule  $qd \times 5/w \times 2w$ . To evaluate the antitumor activity, tumor diameters were measured biweekly with a Vernier caliper. The formula  $TV (\text{mm}^3) = [\text{length} (\text{mm}) \times \text{width} (\text{mm})^2]/2$  was used, where the width and the length are the shortest and the longest diameters of each tumor, respectively. When tumors reached a volume of  $1 \text{ cm}^3$ , mice were sacrificed by cervical dislocation. Body weight was recorded every day throughout the study. Toxicity of the molecules was determined as follows: body weight loss percent ( $\% \text{BWL}_{\text{max}}$ ) =  $100 - [(\text{mean BW}_x / \text{mean BW}_1) \times 100]$ , where  $\text{BW}_x$  is the mean BW at the day of maximal loss during the treatment and  $\text{BW}_1$  is the mean BW on the first day of treatment. Lethal toxicity was also evaluated. Doubling time (DT) of control tumors was also calculated.

In order to assess the effect in vivo of 73, compared to the reference compound 10 (NVP-AUY922), on the expression of typical Hsp90 client proteins, A431 tumor xenografts (3 samples/group) were excised 2 h after the last treatment and then total proteins were extracted through the homogenization of tumor samples in T-PER tissue protein extraction reagent (Pierce, Rockland, IL, U.S.), supplemented with  $10 \mu\text{g/mL}$  protease inhibitor cocktail (Sigma Chemical Co., St. Louis, MO, U.S.). Determination of the protein concentration and Western blotting analysis were finally performed as described in the section Client Protein Degradation Assay.

**Cellular Sensitivity to Drugs.** In non-small-cell lung carcinoma cells (NCI-H460) and in epidermoid carcinoma cells (A431), cellular sensitivity to drugs was evaluated by growth-inhibition assay after 72 h of drug exposure. Cells in the logarithmic phase of growth were seeded into 96-well plates, and 24 h after seeding, the drug was added to the medium. Cell survival was evaluated after 72 h of drug exposure by the sulforhodamine B test.  $\text{IC}_{50}$  was calculated by the ALLFIT program and was defined as the drug concentration causing a 50% reduction of cell number compared to that of untreated control cells.

**Binding on Hsp90 by a Fluorescence Polarization Assay.**<sup>50</sup> GM-FITC, supplied by Invivogen (catalog no. 06C23-MT, CA, U.S.) was previously dissolved in DMSO to obtain 10 mM stock solutions and kept at  $-20^\circ\text{C}$  until use. Hsp90, purchased from Stressgen (catalog no. SPP-776, Victoria, BC, Canada), was previously dissolved in assay buffer (HFB) to form  $2.2 \mu\text{M}$  stock solutions and kept at  $-80^\circ\text{C}$  until use.

The compounds were previously dissolved in DMSO to obtain stock solutions and kept at  $-20^\circ\text{C}$ . On the day of the experiment, various concentration solutions were prepared by serial dilutions in assay buffer (HFB) containing 20 mM HEPES (K), pH 7.3, 50 mM KCl, 5 mM  $\text{MgCl}_2$ , 20 mM  $\text{Na}_2\text{MoO}_4$ , and 0.01% NP40. Before each use, 0.1 mg/mL bovine  $\gamma$  globulin and 2 mM DTT were freshly added. Fluorescence polarization (FP) was performed in Opti-Plate-96F well plates (Perkin-Elmer, Zaventem, Belgium) using a plate reader (Wallac Envision 2101 multilabel reader, Perkin-Elmer, Zaventem, Belgium). To evaluate the binding affinity of the molecules, an amount of  $50 \mu\text{L}$  of the GM-FITC solution (5 nM) was added to 30 nM Hsp90 in the presence of  $5 \mu\text{L}$  of the test compounds at increasing concentrations. The plates were shaken at  $4^\circ\text{C}$  for 4 h, and the FP values in mP (millipolarization units) were recorded. The  $\text{IC}_{50}$  values were calculated as the inhibitor concentration that displaced 50% of the tracer, each data point being the result of the average of triplicate wells, and were determined from a plot using nonlinear least-squares analysis. Curve fitting was performed using Prism GraphPad software program (GraphPad Software, Inc., San Diego, CA, U.S.).

**Client Protein Degradation Assay.** Client protein degradation was determined by Western blotting. Twenty-four hours after seeding on Petri dishes, A431 (human epidermoid carcinoma) cells were treated, for 24 h in complete medium, with various concentrations of test compounds depending on their relative potency. 17-DMAG (at  $0.2 \mu\text{M}$ ) was used as internal reference inhibitor. Following treatments, cells were rinsed twice with ice-cold PBS and lysed in RIPA buffer supplemented with protease and phosphatase inhibitors. After

determination of the protein concentration by Bradford protein assay (Thermo Scientific, Rockford, IL, U.S.), equal amounts of cellular extracts were separated by SDS gel electrophoresis (SDS-PAGE), transferred onto nitrocellulose membranes, and probed with the following primary antibodies: anti-EGFR (Upstate Biotechnology, Millipore Corporate, Billerica, MA, U.S.), anti-Cdk4 (Santa Cruz Biotechnology Inc., CA, U.S.), anti-Akt (Cell Signaling Technology, Inc., MA, U.S.), anti-Hsp70 (BRM-22), and anti-actin (Sigma Chemical Co., St. Louis, MO, U.S.).

Immunoreactive bands were revealed by horseradish peroxidase conjugated secondary antibodies, using an enhanced chemiluminescence detection reagent (ECL Plus, GE Healthcare Bio-Sciences, Uppsala, Sweden) and a specific image system (STORM 860; Molecular Dynamics, Sunnyvale, CA, U.S.). Protein loading equivalence was corrected in relation to the expression of  $\beta$ -actin. For quantification of signals, blots were subjected to densitometry analysis.

**Chemistry.** Reagents were purchased from commercial suppliers and used without further purification.  $^1\text{H}$  NMR spectra were recorded, unless otherwise indicated, in DMSO solution at 200 MHz on a Bruker AC-200, 300 MHz on a Varian Gemini-300, 400 MHz on a Varian Mercury Plus 400 and 500 MHz on a Varian Gemini-500 spectrometer, and peak positions are given in parts per million downfield from tetramethylsilane as the internal standard.  $J$  values are expressed in hertz. Electrospray mass spectra were recorded on a Waters Micromass ZQ-2000 instrument or a double-focusing Finnigan MAT 95 instrument with BE geometry.

Thin layer chromatography (TLC) was carried out using Merck precoated silica gel F-254 plates. Flash chromatography was done using Merck silica gel 60 (0.063–0.200 mm). Solvents were dried according to standard procedures, and reactions requiring anhydrous conditions were performed under argon. Solutions containing the final products were dried with  $\text{Na}_2\text{SO}_4$ , filtered, and concentrated under reduced pressure using a rotatory evaporator. All the final products undergoing biological testing were analyzed in a Jasco HPLC system consisting of two PU-2080 pumps and an MD-2010 detector. A purity threshold of 98% was set up. Microanalysis of all new synthesized compounds indicated values were within  $\pm 0.4\%$  of the calculated value.

**General Procedure for the Synthesis of Nitroisoxazoles 13a–d.** A suspension of adequate isoxazole derivative 12a–d (2.2 mmol) in  $\text{Ac}_2\text{O}$  (20 mL) was cooled to  $0^\circ\text{C}$ , and concentrated  $\text{HNO}_3$  (0.26 mL, 4.3 mmol) was added dropwise under stirring, the temperature being maintained between  $0$  and  $5^\circ\text{C}$ . After the addition was complete, the mixture was stirred for 70 h at  $5$ – $10^\circ\text{C}$  and then poured into ice and extracted with DCM ( $3 \times 40 \text{ mL}$ ). The extract was dried and concentrated under vacuo. The yellow solid obtained was triturated with  $\text{Et}_2\text{O}$  and filtered to give the desired nitro compound 13a–d.

**5-[2,4-Bis(benzyloxy)-5-chlorophenyl]-4-nitroisoxazole-3-carboxylic Acid Ethylamide (13a).** Yield 73%. Yellow solid.  $^1\text{H}$  NMR (200 MHz  $\text{CDCl}_3$ )  $\delta$ : 1.26 (t,  $J = 7.4 \text{ Hz}$ , 3H), 3.46–3.55 (m, 2H), 5.0 (s, 2H), 5.10 (s, 2H), 6.57 (m, 2H), 7.23–7.29 (m, 2H), 7.32–7.37 (m, 8H), 7.66 (s, 1H).  $m/z$  508.5/510.4  $[\text{M} + \text{H}]^+$ .

**5-[2,4-Bis(benzyloxy)-5-chlorophenyl]-*N*-(2,2,2-trifluoroethyl)-4-nitroisoxazole-3-carboxamide (13b).** Yellow solid.  $^1\text{H}$  NMR (400 MHz  $\text{CDCl}_3$ )  $\delta$ : 4.07–4.15 (m, 2H), 5.01 (s, 2H), 5.10 (s, 2H), 6.59 (s, 1H), 6.93 (br, 1H), 7.22–7.27 (m, 2H), 7.32–7.40 (m, 8H), 7.68 (s, 1H).  $m/z$  562.5/564.4  $[\text{M} + \text{H}]^+$ .

**5-[2,4-Bis(benzyloxy)-5-chlorophenyl]-4-nitroisoxazol-3-yl)-(3,3-difluoroazetid-1-yl)methanone (13c).** Yellow solid.  $^1\text{H}$  NMR (400 MHz  $\text{CDCl}_3$ )  $\delta$ : 4.52–4.58 (m, 4H), 4.99 (s, 2H), 5.14 (s, 2H), 6.62 (s, 1H), 7.25–7.27 (m, 2H), 7.35–7.41 (m, 8H), 7.66 (s, 1H).  $m/z$  556.5/558.4  $[\text{M} + \text{H}]^+$ .

**5-[2,4-Bis(benzyloxy)-5-isopropylphenyl]-4-nitroisoxazole-3-carboxylic Acid Ethylamide (13d).** Yellow solid.  $^1\text{H}$  NMR (200 MHz  $\text{CDCl}_3$ )  $\delta$ : 1.22–1.26 (m, 9H), 3.24–3.38 (m, 1H), 3.43–3.57 (m, 2H), 5.02 (s, 4H), 6.54 (s, 1H), 6.59 (br, 1H), 7.30–7.39 (m, 10H), 7.46 (s, 1H).  $m/z$  516.5  $[\text{M} + \text{H}]^+$ .

**General Procedure To Obtain the 4-Aminoisoxazoles 14a–d.** A solution of the appropriate nitro derivative 13a–d (1.97 mmol) in THF (7 mL) was added to a solution of  $\text{NH}_4\text{Cl}$  (2.7 g, 50 mmol) in water (15 mL). Zinc dust (4 g, 61 mmol) was then added portionwise over 15 min with stirring at 0 °C. After 30 min at 0 °C, the mixture was filtered and the resulting cake was rinsed with MeOH. The combined filtrate was evaporated in vacuo to give the desired amino compounds 14a–d.

**4-Amino-5-[2,4-bis(benzyloxy)-5-chlorophenyl]isoxazole-3-carboxylic Acid Ethylamide (14a).** Yield 82%. Yellow solid.  $^1\text{H}$  NMR (200 MHz  $\text{CDCl}_3$ )  $\delta$ : 1.24 (t,  $J = 7.2$  Hz, 3H), 3.38–3.53 (m, 2H), 5.02 (s, 2H), 5.15 (s, 2H), 6.64 (s, 1H), 6.79 (br, 1H), 7.35–7.42 (m, 10H), 7.64 (s, 1H).  $m/z$  478.3/480.4  $[\text{M} + \text{H}]^+$ .

**5-[2,4-Bis(benzyloxy)-5-chlorophenyl]-4-amino-N-(2,2,2-trifluoroethyl)isoxazole-3-carboxamide (14b).** Yield 77%. Yellow solid.  $^1\text{H}$  NMR (200 MHz  $\text{CDCl}_3$ )  $\delta$ : 3.97–4.14 (m, 2H), 4.35 (br, 2H), 5.04 (s, 2H), 5.16 (s, 2H), 6.65 (s, 1H), 7.08 (br, 1H), 7.31–7.44 (m, 10H), 7.65 (s, 1H).  $m/z$  532.3/534.3  $[\text{M} + \text{H}]^+$ .

**5-[2,4-Bis(benzyloxy)-5-chlorophenyl]-4-aminoisoxazol-3-yl-(3,3-difluoroazetidin-1-yl)methanone (14c).** Yield 65%. Yellow solid.  $^1\text{H}$  NMR (200 MHz  $\text{CDCl}_3$ )  $\delta$ : 4.43–4.55 (m, 4H), 4.83–4.95 (m, 2H), 5.03 (s, 2H), 5.15 (s, 2H), 6.64 (s, 1H), 7.29–7.43 (m, 10H), 7.64 (s, 1H).  $m/z$  526.4/528.5  $[\text{M} + \text{H}]^+$ .

**4-Amino-5-[2,4-bis(benzyloxy)-5-isopropylphenyl]isoxazole-3-carboxylic Acid Ethylamide (14d).** Yield 72%. Yellow solid.  $^1\text{H}$  NMR (200 MHz  $\text{CDCl}_3$ )  $\delta$ : 1.21–1.28 (m, 9H), 3.28–3.38 (m, 1H), 3.39–3.53 (m, 2H), 4.38 (br, 2H), 5.05 (s, 2H), 5.08 (s, 2H), 6.61 (s, 1H), 6.83 (br, 1H), 7.33–7.42 (m, 10H), 7.45 (s, 1H).  $m/z$  486.6  $[\text{M} + \text{H}]^+$ .

**General Procedure for Preparation of 4-Isioxazole Amides 15–73.** A solution of the appropriate amine 14a–d (1.45 mmol) and TEA (1.74 mmol, 0.24 mL) in DCM was added dropwise to a solution of the corresponding acyl chloride (1.45 mmol). The mixture was stirred for 5 h, diluted with DCM, and washed with 1 N HCl. The organic extract was dried and filtered. Solvents were removed in vacuo to give the crude residue that was used without further purification. The amide thus obtained (0.35 mmol) was dissolved in DCM (10 mL) and was cooled under an inert atmosphere at 0 °C, and  $\text{BCl}_3$  in 1 M DCM (1.05 mmol, 1.05 mL) was added dropwise. The mixture was stirred at 0 °C for 20 min. The cooling bath was then removed and the mixture left for a further 50 min at room temperature. The mixture was cooled again and then quenched by cautious addition of saturated aqueous  $\text{NaHCO}_3$  solution (20 mL). The DCM was removed in vacuo, and water (20 mL) was added. The mixture was then extracted with EtOAc (200 mL). The organic layers were washed with water (2  $\times$  30 mL), saturated aqueous NaCl solution (50 mL) and then dried over  $\text{Na}_2\text{SO}_4$ . Crude products were purified by flash chromatography on silica gel (yield, 35–60%).

**5-(5-Chloro-2,4-dihydroxyphenyl)-4-[(3-methylthiophene-2-carbonyl)amino]isoxazole-3-carboxylic Acid Ethylamide (19).** Light-yellow solid.  $^1\text{H}$  NMR (400 MHz)  $\delta$ : 1.09 (t,  $J = 6.8$  Hz, 3H), 2.43 (s, 3H), 3.20–3.25 (m, 2H), 6.65 (s, 1H), 7.01 (d,  $J = 5.2$  Hz, 1H), 7.44 (s, 1H), 7.66 (d,  $J = 5.2$  Hz, 1H), 8.58 (t,  $J = 5.6$  Hz, 1H), 9.29 (br, 1H), 10.70 (s, 2H).  $m/z$  422.1/424.1  $[\text{M} + \text{H}]^+$ . Anal. ( $\text{C}_{18}\text{H}_{16}\text{ClN}_3\text{O}_5\text{S}$ ) C, H, Cl, N, S.

**5-(5-Chloro-2,4-dihydroxyphenyl)-4-(2,2-dimethylpropionylamino)isoxazole-3-carboxylic Acid Ethylamide (21).** White solid.  $^1\text{H}$  NMR (400 MHz)  $\delta$ : 1.06 (t,  $J = 7.2$  Hz, 3H), 1.14 (s, 9H), 3.19–3.24 (m, 2H), 6.66 (s, 1H), 7.34 (s, 1H), 8.58 (t,  $J = 5.6$  Hz, 1H), 8.83 (s, 1H), 10.50 (br, 1H), 10.70 (s, 1H).  $m/z$  382.2/384.2  $[\text{M} + \text{H}]^+$ . Anal. ( $\text{C}_{17}\text{H}_{20}\text{ClN}_3\text{O}_5\text{S}$ ) C, H, Cl, N.

**4-[(Adamantane-1-carbonyl)amino]-5-(5-chloro-2,4-dihydroxyphenyl)isoxazole-3-carboxylic Acid Ethylamide (23).** White solid.  $^1\text{H}$  NMR (400 MHz)  $\delta$ : 1.09 (t,  $J = 7.2$  Hz, 3H), 1.65–1.69 (m, 6H), 1.81–1.82 (m, 6H), 1.99 (s, 3H), 3.18–3.24 (m, 2H), 6.67 (s, 1H), 7.34 (s, 1H), 8.74 (t,  $J = 5.6$  Hz, 1H), 10.55 (br, 2H).  $m/z$  460.2/462.3  $[\text{M} + \text{H}]^+$ . Anal. ( $\text{C}_{23}\text{H}_{26}\text{ClN}_3\text{O}_5$ ) C, H, Cl, N.

**4-Acetylamino-5-(2,4-dihydroxy-5-isopropylphenyl)isoxazole-3-carboxylic Acid Ethylamide (26).** White solid.  $^1\text{H}$  NMR (400 MHz)  $\delta$ : 1.07–1.12 (m, 9H), 3.06–3.13 (m, 1H), 3.21–3.26 (m, 2H), 6.49 (s, 1H), 7.11 (s, 1H), 8.55 (t,  $J = 6.0$  Hz, 1H), 9.15

(br, 1H), 9.81 (s, 1H), 9.90 (br, 1H).  $m/z$  348.5  $[\text{M} + \text{H}]^+$ . Anal. ( $\text{C}_{17}\text{H}_{21}\text{N}_3\text{O}_5$ ) C, H, N.

**5-(2,4-Dihydroxy-5-isopropylphenyl)-4-(2,2-dimethylpropionylamino)isoxazole-3-carboxylic Acid Ethylamide (27).** White solid.  $^1\text{H}$  NMR (400 MHz  $\text{CD}_3\text{OD}$ )  $\delta$ : 1.18–1.24 (m, 18H), 3.17–3.24 (m, 1H), 3.48 (q,  $J = 6.8$  Hz, 2H), 6.47 (s, 1H), 7.27 (s, 1H).  $m/z$  390.5  $[\text{M} + \text{H}]^+$ . Anal. ( $\text{C}_{20}\text{H}_{27}\text{N}_3\text{O}_5$ ) C, H, N.

**4-(Cyclohexanecarbonylamino)-5-(2,4-dihydroxy-5-isopropylphenyl)isoxazole-3-carboxylic Acid Ethylamide (28).**  $^1\text{H}$  NMR (300 MHz)  $\delta$ : 1.06 (t,  $J = 5.1$  Hz, 3H), 1.08 (d,  $J = 7.2$  Hz, 6H), 1.10–1.36 (m, 5H), 1.57–1.77 (m, 5H), 2.23 (m, 1H), 3.06 (m, 1H), 3.19 (m, 2H), 6.47 (s, 1H), 7.09 (s, 1H), 8.46 (t,  $J = 6.3$  Hz, NH), 8.97 (s, OH), 9.77 (s, NH), 9.89 (s, OH).  $m/z$  438.0  $[\text{M} + \text{Na}]^+$ . Anal. ( $\text{C}_{22}\text{H}_{29}\text{N}_3\text{O}_5$ ) C, H, N.

**5-(2,4-Dihydroxy-5-isopropylphenyl)-4-[(cis-4-methoxycyclohexanecarbonyl)amino]isoxazole-3-carboxylic Acid Ethylamide (31).**  $^1\text{H}$  NMR (300 MHz)  $\delta$ : 1.07 (t,  $J = 5.2$  Hz, 3H), 1.09 (d,  $J = 7.3$  Hz, 6H), 1.37 (m, 2H), 1.49 (m, 2H), 1.61 (m, 2H), 1.80 (m, 2H), 2.26 (m, 1H), 3.06 (m, 1H), 3.14 (s, 3H), 3.16 (m, 2H), 3.29 (bs, 1H), 6.47 (s, 1H), 7.09 (s, 1H), 8.47 (t,  $J = 6.2$  Hz, 1H), 8.9 (s, 1H), 9.76 (s, 1H), 9.85 (s, 1H).  $m/z$  468.3  $[\text{M} + \text{Na}]^+$ . Anal. ( $\text{C}_{23}\text{H}_{31}\text{N}_3\text{O}_6$ ) C, H, N.

**(15,3R)-3-[5-(2,4-Dihydroxy-5-isopropylphenyl)-3-ethylcarbamoylisoxazol-4-ylcarbamoyl]cyclopentanecarboxylic Acid Methyl Ester (43).**  $^1\text{H}$  NMR (300 MHz)  $\delta$ : 1.06 (t,  $J = 7.0$  Hz, 3H), 1.08 (d,  $J = 6.7$  Hz, 6H), 1.76–1.90 (m, 4H), 2.03–2.12 (m, 2H), 2.75–2.79 (m, 2H), 3.06 (hept,  $J = 7.0$  Hz, 1H), 3.19 (q,  $J = 7.0$  Hz, 2H), 3.56 (s, 3H), 6.48 (s, 1H), 7.08 (s, 1H), 8.49 (t,  $J = 5.5$  Hz, 1H), 9.12 (bs, 1H), 9.78 (bs, 2H).  $m/z$  459.9  $[\text{M} + \text{H}]^+$ . Anal. ( $\text{C}_{23}\text{H}_{29}\text{N}_3\text{O}_7$ ) C, H, N.

**5-(2,4-Dihydroxy-5-isopropylphenyl)-4-(4-methoxybenzoylamino)isoxazole-3-carboxylic Acid Ethylamide (46).** White solid.  $^1\text{H}$  NMR (400 MHz)  $\delta$ : 1.04–1.28 (m, 9H), 3.03–3.08 (m, 1H), 3.19–3.23 (m, 2H), 3.82 (s, 3H), 6.47 (s, 1H), 7.02 (d,  $J = 8.8$  Hz, 2H), 7.23 (s, 1H), 7.87 (d,  $J = 8.8$  Hz, 2H), 8.61 (t,  $J = 5.6$  Hz, 1H), 9.56 (br, 1H), 9.82 (s, 1H), 10.08 (br, 1H).  $m/z$  440.4  $[\text{M} + \text{H}]^+$ . Anal. ( $\text{C}_{23}\text{H}_{25}\text{N}_3\text{O}_6$ ) C, H, N.

**5-(2,4-Dihydroxy-5-isopropylphenyl)-4-(4-morpholin-4-ylmethylbenzoylamino)isoxazole-3-carboxylic Acid Ethylamide (49).**  $^1\text{H}$  NMR (300 MHz)  $\delta$ : 1.04 (d,  $J = 7.2$  Hz, 6H), 1.07 (t,  $J = 7.0$  Hz, 3H), 3.18–3.22 (m, 4H), 3.02–3.09 (m, 3H), 3.78 (m, 2H), 3.89 (m, 2H), 4.38 (bs, 2H), 6.52 (s, 1H), 7.21 (s, 1H), 7.73 (d,  $J = 7.3$  Hz, 2H), 7.96 (d,  $J = 7.3$  Hz, 2H), 8.64 (t,  $J = 5.8$  Hz, 1H), 9.76 (s, 1H), 9.86 (s, 1H), 10.13 (s, 1H), 11.2 (s, 1H).  $m/z$  530.8  $[\text{M} + \text{Na}]^+$ . Anal. ( $\text{C}_{27}\text{H}_{32}\text{N}_4\text{O}_6$  HCl) C, H, N.

**5-(2,4-Dihydroxy-5-isopropylphenyl)-4-(5-ethylisoxazole-3-carbonyl)aminoisoxazole-3-carboxylic Acid Ethylamide (55).** White solid.  $^1\text{H}$  NMR (400 MHz  $\text{CD}_3\text{OD}$ )  $\delta$ : 1.18–1.31 (m, 12H), 2.80–2.86 (m, 2H), 3.16–3.22 (m, 1H), 3.39 (q,  $J = 7.2$  Hz, 2H), 6.47 (s, 1H), 6.48 (s, 1H), 7.33 (s, 1H).  $m/z$  429.0  $[\text{M} + \text{H}]^+$ . Anal. ( $\text{C}_{21}\text{H}_{24}\text{N}_4\text{O}_6$ ) C, H, N.

**5-(2,4-Dihydroxy-5-isopropylphenyl)-4-[(3-methylthiophene-2-carbonyl)amino]isoxazole-3-carboxylic Acid Ethylamide (57).** White solid.  $^1\text{H}$  NMR (400 MHz)  $\delta$ : 1.07–1.11 (m, 9H), 2.44 (s, 3H), 3.05–3.11 (m, 1H), 3.19–3.25 (m, 2H), 6.52 (s, 1H), 7.01 (d,  $J = 5.2$  Hz, 1H), 7.22 (s, 1H), 7.66 (d,  $J = 5.2$  Hz, 1H), 8.66 (t,  $J = 5.6$  Hz, 1H), 9.12 (s, 1H), 9.89 (s, 1H), 10.22 (br, 1H).  $m/z$  430.6  $[\text{M} + \text{H}]^+$ . Anal. ( $\text{C}_{21}\text{H}_{23}\text{N}_3\text{O}_5\text{S}$ ) C, H, N, S.

**4-[(5-Bromofuran-2-carbonyl)amino]-5-(2,4-dihydroxy-5-isopropylphenyl)isoxazole-3-carboxylic Acid Ethylamide (58).**  $^1\text{H}$  NMR (300 MHz)  $\delta$ : 1.05 (d,  $J = 7.0$  Hz, 6H), 1.07 (t,  $J = 7.6$  Hz, 3H), 3.05 (hept,  $J = 6.7$  Hz, 1H), 3.21 (quint,  $J = 7.6$  Hz, 2H), 6.47 (s, 1H), 6.78 (d,  $J = 3.7$  Hz, 1H), 7.17 (s, 1H), 7.24 (d,  $J = 3.7$  Hz, 1H), 8.62 (t,  $J = 5.7$  Hz, 1H), 9.75 (bs, 1H), 9.81 (s, 1H), 10.08 (bs, 1H).  $m/z$  477.3/479.3  $[\text{M} - \text{H}]^-$ . Anal. ( $\text{C}_{20}\text{H}_{20}\text{BrN}_3\text{O}_6$ ) C, H, N.

**5-(2,4-Dihydroxy-5-isopropylphenyl)-4-[(furan-2-carbonyl)amino]isoxazole-3-carboxylic Acid Ethylamide (71).**  $^1\text{H}$  NMR (300 MHz)  $\delta$ : 1.06 (d,  $J = 7.0$  Hz, 6H), 1.08 (t,  $J = 7.5$  Hz, 3H), 3.06 (m, 1H), 3.21 (m, 2H), 6.49 (s, H), 6.65 (dd,  $J = 1.6$  Hz,  $J = 3.5$  Hz, 1H), 7.19 (s, 1H), 7.2 (d,  $J = 3.5$  Hz, 1H), 7.88 (d,  $J = 1.6$  Hz, 1H),

8.62 (t,  $J = 5.4$  Hz, 1H), 9.5 (s, 1H), 9.83 (s, 1H), 10.2 (s, 1H).  $m/z$  400.3  $[M + H]^+$ . Anal. ( $C_{20}H_{21}N_3O_6$ ) C, H, N.

**5-(2,4-Dihydroxy-5-isopropylphenyl)-4-(5-(morpholinomethyl)isoxazole-3-carboxylamino)isoxazole-3-carboxylic Acid Ethylamide (73).**  $^1H$  NMR (400 MHz  $CD_3OD$ ),  $\delta$ : 1.18–1.26 (m, 9H), 2.52–2.54 (m, 4H), 3.17–3.25 (m, 1H), 3.39 (q,  $J = 7.2$  Hz, 2H), 3.68–3.70 (m, 4H), 3.78 (s, 1H), 6.47 (s, 1H), 6.72 (s, 1H), 7.34 (s, 1H).  $m/z$  499.9  $[M + H]^+$ . Anal. ( $C_{24}H_{29}N_5O_7$ ) C, H, N.

## ■ ASSOCIATED CONTENT

### Supporting Information

Additional experimental procedures and characterization data, docking studies, analysis of the degradation of Hsp90 client proteins, physicochemical parameters of 60 compounds, and metabolism data. This material is available free of charge via the Internet at <http://pubs.acs.org>.

## ■ AUTHOR INFORMATION

### Corresponding Author

\*For D.S.: phone, +39-0532-455923; fax, +39-0532-455953; e-mail, [smd@unife.it](mailto:smd@unife.it). For G.G.: phone, +39-0691393640; fax, +39-0691393638; e-mail, [giuseppe.giannini@sigma-tau.it](mailto:giuseppe.giannini@sigma-tau.it).

## ■ ACKNOWLEDGMENTS

The authors thank Isabella Lustrati, Silvio Zavatto, M. Cati, Massimo De Santis, Federico Serafini, and Virgilio Achermann for excellent technical assistance. This work was supported by grants from Sigma-Tau Research Switzerland S.A. (P.O. Box 1823, Via Motta 2a-CH-6850 Mendrisio, Switzerland; phone, +41-091640.4050).

## ■ DEDICATION

<sup>†</sup>Dedicated to the memory of Dr. Paolo Carminati.

## ■ ABBREVIATIONS USED

Hsp90, heat shock protein 90; 17-AAG, 17-allylaminogeldanamycin; 17-DMAG, 17-dimethylaminoethylamino-17-demethoxygeldanamycin; TVI, tumor volume inhibition; BWL, body weight loss

## ■ REFERENCES

- (1) Maloney, A.; Workman, P. Hsp90 as a new therapeutic target for cancer therapy: the story unfolds. *Expert Opin. Biol. Ther.* **2002**, *2*, 3–24.
- (2) Whitesell, L.; Lindquist, S. L. Hsp90 and the chaperoning of cancer. *Nat. Rev. Cancer* **2005**, *5*, 761–772.
- (3) Kamal, A.; Boehm, M. F.; Burrows, F. J. Therapeutic and diagnostic implications of Hsp90 activation. *Trends Mol. Med.* **2004**, *10*, 283–290.
- (4) Pratt, W. B.; Morishima, Y.; Peng, H.-M.; Osawa, Y. Proposal for a role of the Hsp90/Hsp70-based chaperone machinery in making triage decisions when proteins undergo oxidative and toxic damage. *Exp. Biol. Med.* **2010**, *235*, 278–289.
- (5) Vega, V. L.; De Maio, A. Geldanamycin treatment ameliorates the response to LPS in murine macrophages by decreasing CD14 surface expression. *Mol. Biol. Cell* **2003**, *14*, 764–773.
- (6) Poulaki, V.; Iliaki, E.; Mitsiades, N.; Mitsiades, C. S.; Paulus, Y. N.; Bula, D. V.; Gragoudas, E. S.; Miller, J. W. Inhibition of Hsp90 attenuates inflammation in endotoxin-induced uveitis. *FASEB J.* **2007**, *21*, 2113–2123.
- (7) Kumar, R.; Pavithra, S. R.; Tatu, U. Three-dimensional structure of heat shock protein 90 from *Plasmodium falciparum*: molecular modelling approach to rational drug design against malaria. *J. Biosci.* **2007**, *32*, 531–536.

(8) Solit, D. B.; Chiosis, G. Development and application of Hsp90 inhibitors. *Drug Discovery Today* **2008**, *13c*, 38–43.

(9) Prodromou, C.; Peral, L. H. Structure and functional relationship of the Hsp90. *Curr. Cancer Drug Targets* **2003**, *3*, 301–323.

(10) Cowena, L. E.; Singha, S. D.; Köhler, J. R.; Collins, C.; Zaas, A. K.; Schell, W. A.; Aziz, H.; Mylonakis, E.; Perfect, J. R.; Whitesell, L.; Lindquist, S. Harnessing Hsp90 function as a powerful, broadly effective therapeutic strategy for fungal infectious disease. *Proc. Natl. Acad. Sci. U.S.A.* **2009**, *106*, 2818–2823.

(11) Connor, J. H.; McKenzie, M. O.; Parks, G. D.; Lyles, D. S. Antiviral activity and RNA polymerase degradation following Hsp90 inhibition in a range of negative strand viruses. *Virology* **2007**, *362*, 109–119.

(12) Luo, W.; Dou, F.; Rodina, A.; Chip, S.; Kim, J.; Zhao, Q.; Moullick, K.; Aguirre, J.; Wu, N.; Greengard, P.; Chiosis, G. Roles of heat-shock protein 90 in maintaining and facilitating the neurodegenerative phenotype in tauopathies. *Proc. Natl. Acad. Sci. U.S.A.* **2007**, *104*, 9511–9516.

(13) Zhang, H.; Burrows, F. Targeting multiple signal transduction pathways through inhibition of Hsp90. *J. Mol. Med.* **2004**, *82*, 488–499.

(14) Workman, P. Combinatorial attack on multistep oncogenesis by inhibiting the Hsp90 molecular chaperone. *Cancer Lett.* **2004**, *206*, 149–157.

(15) Vilenchik, M.; Solit, D.; Basso, A.; Huez, H.; Lucas, B.; He, H.; Rosen, N.; Spampinato, C.; Modrich, P.; Chiosis, G. Targeting wide-range oncogenic transformation via PU24FCL, a specific inhibitor of tumor Hsp90. *Chem. Biol.* **2004**, *11*, 787–797.

(16) Csermely, P.; Schnaider, T.; Soti, C.; Prohászka, Z.; Nardai, G. The 90-kDa molecular chaperone family: structure, function, and clinical applications. A comprehensive review. *Pharmacol. Ther.* **1998**, *79*, 129–168.

(17) Stravopodis, D. J.; Margaritis, L. H.; Voutsinas, G. E. Drug-mediated targeted disruption of multiple protein activities through functional inhibition of the Hsp90 chaperone complex. *Curr. Med. Chem.* **2007**, *14*, 3122–3138.

(18) Whitesell, L.; Lindquist, S. L. HSP90 and the chaperoning of cancer. *Nat. Rev. Cancer* **2005**, *5*, 761–772.

(19) Picard, D. Heat-shock protein 90, a chaperone for folding and regulation. *Cell. Mol. Life Sci.* **2002**, *59*, 1640–1648.

(20) Eustace, B. K.; Sakurai, T. A.; Stewart, J. K.; Yimlamai, D.; Unger, C.; Zehetmeier, C.; Lain, B.; Torella, C.; Henning, S. W.; Beste, G.; Scroggins, B. T.; Neckers, L.; Ilag, L. L.; Jay, D. G. Functional proteomic screens reveal an essential extracellular role for hsp90 alpha in cancer cell invasiveness. *Nat. Cell Biol.* **2004**, *6*, 507–514.

(21) Koga, F.; Tsutsumi, S.; Neckers, L. M. Low dose geldanamycin inhibits hepatocyte growth factor and hypoxia-stimulated invasion of cancer cells. *Cell Cycle* **2007**, *6*, 1393–1402.

(22) Trepel, J.; Mollapour, M.; Giaccone, G.; Neckers, L. Targeting the dynamic HSP90 complex in cancer. *Nat. Rev. Cancer* **2010**, *10*, 537–549.

(23) Whitesell, L.; Shifrin, S. D.; Schwab, G.; Neckers, L. M. Benzoquinonoid ansamycins possess selective tumoricidal activity unrelated to src kinase inhibition. *Cancer Res.* **1992**, *52*, 1721–1728.

(24) Supko, J. G.; Hickman, R. L.; Grever, M. R.; Malspeis, L. Preclinical pharmacologic evaluation of geldanamycin as an antitumor agent. *Cancer Chemother. Pharmacol.* **1995**, *36*, 305–315.

(25) Infinity Pharmaceuticals, Inc. Product Candidates. <http://www.infi.com/product-candidates-pipeline.asp>.

(26) Sharma, S. V.; Agatsuma, T.; Nakano, H. Targeting of the protein chaperone, HSP90, by the transformation suppressing agent, radicicol. *Oncogene* **1998**, *16*, 2639–2645.

(27) Biamonte, M. A.; Van de Water, R.; Arndt, J. W.; Scannevin, R. H.; Perret, D.; Lee, W.-C. Heat shock protein 90: inhibitors in clinical trials. *J. Med. Chem.* **2010**, *53*, 3–17.

(28) Holzbeierlein, J. M.; Windsperger, A.; Vielhauer, G. Hsp90: a drug target? *Curr. Oncol. Rep.* **2010**, *12*, 95–101.

(29) Taldone, T.; Chiosis, G. Purine-scaffold Hsp90 inhibitors. *Curr. Top. Med. Chem.* **2009**, *9*, 1436–1446.

- (30) He, H.; Zatorska, D.; Kim, J.; Aguirre, J.; Llauger, L.; She, Y.; Wu, N.; Immormino, R. M.; Gewirth, D. T.; Chiosis, G. Identification of potent water soluble purine-scaffold inhibitors of the heat shock protein 90. *J. Med. Chem.* **2006**, *49*, 381–390.
- (31) Debiopharm Group. Pipeline. [www.debiopharm.com/our-business/pipeline.html](http://www.debiopharm.com/our-business/pipeline.html).
- (32) Huang, K. H.; Veal, J. M.; Fadden, R. P.; Rice, J. W.; Eaves, J.; Strachan, J.-P.; Barabasz, A. F.; Foley, B. E.; Barta, T. E.; Ma, W.; Silinski, M. A.; Hu, M.; Partridge, J. M.; Scott, A.; DuBois, L. G.; Freed, T.; Steed, P. M.; Ommen, A. J.; Smith, E. D.; Hughes, P. F.; Woodward, A. R.; Hanson, G. J.; McCall, W. S.; Markworth, C. J.; Hinkley, L.; Jenks, M.; Geng, L.; Lewis, M.; Otto, J.; Pronk, B.; Verleysen, K.; Hall, S. E. Discovery of novel 2-aminobenzamide inhibitors of heat shock protein 90 as potent, selective and orally active antitumor agents. *J. Med. Chem.* **2009**, *52*, 4288–4305.
- (33) Gopalsamy, A.; Shi, M.; Golas, J.; Vogan, E.; Jacob, J.; Johnson, M.; Lee, F.; Nilakantan, R.; Petersen, R.; Svenson, K.; Chopra, R.; Tam, M. S.; Wen, Y.; Ellingboe, J.; Arndt, K.; Boschelli, F. Discovery of benzisoxazoles as potent inhibitors of chaperone heat shock protein 90. *J. Med. Chem.* **2008**, *51*, 373–375.
- (34) Woodhead, A. J.; Angove, H.; Carr, M. G.; Chessari, G.; Congreve, M.; Coyle, J. E.; Cosme, J.; Graham, B.; Day, P. J.; Downham, R.; Fazal, L.; Feltell, R.; Figueroa, E.; Frederickson, M.; Lewis, J.; McMenemy, R.; Murray, C. W.; O'Brien, M. A.; Parra, L.; Patel, S.; Phillips, T.; Rees, D. C.; Rich, S.; Smith, D.-M.; Gary Trewartha, G.; Vinkovic, M.; Williams, B.; Woolford, A. J.-A. Discovery of (2,4-dihydroxy-5-isopropylphenyl)-[5-(4-methylpiperazin-1-ylmethyl)-1,3-dihydroisoindol-2-yl]methanone (AT13387), a novel inhibitor of the molecular chaperone Hsp90 by fragment based drug design. *J. Med. Chem.* **2010**, *53*, 5956–5969.
- (35) Wang, Y.; Trepel, J. B.; Neckers, L. M.; Giaccone, G. STA-9090, a small-molecule Hsp90 inhibitor for the potential treatment of cancer. *Curr. Opin. Invest. Drugs* **2010**, *11*, 1466–1476.
- (36) London, C. A.; Bear, M. D.; McCleese, J.; Foley, K. P.; Paalanga, R.; Inoue, T.; Ying, W.; Barsoum, J. Phase I Evaluation of STA-1474, a Pro-Drug of the Novel HSP90 Inhibitor Ganetespib, in Dogs with Spontaneous Cancer. Presented at the 102nd Annual Meeting of the AACR, Orlando, FL, Apr 2–6, 2011; Abstract 1282.
- (37) Papac, D. I.; Patton, J. S.; Reeves, L.; Bulka, K.; DeMie, L.; Roman, O.; Bradford, C.; Kim, S.-H.; Tangallapally, R.; Trovato, R.; Markovitz, B.; Bajji, A.; Wettstein, D.; Baichwal, V.; Mather, G. Comparative in Vitro and in Vivo Metabolism of MPC-3100, an Oral Hsp90 Inhibitor, in Rat, Dog, Monkey and Human. Presented at the 102nd Annual Meeting of the AACR, Orlando, FL, Apr 2–6, 2011; Abstract 3233.
- (38) Papac, D.; Patton, J. S.; Reeves, L.; DeMie, L.; Bradford, C.; Hachey, B.; Clemetson, B.; Christensen, C.; Kim, S.-H.; Tangallapally, R.; Parker, D.; Trovato, R.; Kim, I. C.; Wettstein, D.; Baichwal, V. R.; Bajji, A. Evaluation of the Pharmacokinetics and Efficacy of a Novel Pro-Drug of the Hsp90 Inhibitor, MPC-3100, Designed with Improved Solubility. Presented at the 102nd Annual Meeting of the AACR, Orlando, FL, Apr 2–6, 2011; Abstract 3237.
- (39) Cheung, K. M.; Matthews, T. P.; James, K.; Rowlands, M. G.; Boxall, K. J.; Sharp, S. Y.; Maloney, A.; Roe, S. M.; Prodromou, C.; Pearl, L. H.; Aherne, G. W.; McDonald, E.; Workman, P. The identification, synthesis, protein crystal structure and in vitro biochemical evaluation of a new 3,4-diarylpyrazole class of Hsp90 inhibitors. *Bioorg. Med. Chem. Lett.* **2005**, *15*, 3338–3343.
- (40) Brough, P. A.; Barril, X.; Beswick, M.; Dymock, B. W.; Drysdale, M. J.; Wright, L.; Grant, K.; Massey, A.; Surgenor, A.; Workman, P. 3-(5-Chloro-2,4-dihydroxyphenyl)-pyrazole-4-carboxamides as inhibitors of the Hsp90 molecular chaperone. *Bioorg. Med. Chem. Lett.* **2005**, *15*, 5197–5201.
- (41) Brough, P. A.; Aherne, W.; Barril, X.; Borgognoni, J.; Boxall, K.; Cansfield, J. E.; Cheung, K. M.; Collins, I.; Davies, N. G.; Drysdale, M. J.; Dymock, B.; Eccles, S. A.; Finch, H.; Fink, A.; Hayes, A.; Howes, R.; Hubbard, R. E.; James, K.; Jordan, A. M.; Lockie, A.; Martins, V.; Massey, A.; Matthews, T. P.; McDonald, E.; Northfield, C. J.; Pearl, L. H.; Prodromou, C.; Ray, S.; Raynaud, F. I.; Roughley, S. D.; Sharp, S. Y.; Surgenor, A.; Walmsley, D. L.; Webb, P.; Wood, M.; Workman, P.; Wright, L. 4,5-Diarylisoaxazole Hsp90 chaperone inhibitors: potential therapeutic agents for the treatment of cancer. *J. Med. Chem.* **2008**, *51*, 196–218.
- (42) Dymock, B. W.; Barril, X.; Brough, P. A.; Cansfield, J. E.; Massey, A.; McDonald, E.; Hubbard, R. E.; Surgenor, A.; Roughley, S. D.; Webb, P.; Workman, P.; Wright, L.; Drysdale, M. J. Novel potent small-molecule inhibitors of the molecular chaperone Hsp90 discovered through structure-based design. *J. Med. Chem.* **2005**, *48*, 4212–4215.
- (43) Smith, N. F.; Hayes, A.; James, K.; Nutley, B. P.; McDonald, E.; Henley, A.; Dymock, B.; Drysdale, M. J.; Raynaud, F. I.; Workman, P. Preclinical pharmacokinetics and metabolism of a novel diaryl pyrazole resorcinol series of heat shock protein 90 inhibitors. *Mol. Cancer Ther.* **2006**, *5*, 1628–1638.
- (44) Brough, P. A.; Barril, X.; Borgognoni, J.; Chene, P.; Davies, N. G.; Davis, B.; Drysdale, M. J.; Dymock, B.; Eccles, S. A.; Garcia-Echeverria, C.; Fromont, C.; Hayes, A.; Hubbard, R. E.; Jordan, A. M.; Jensen, M. R.; Massey, A.; Merrett, A.; Padfield, A.; Parsons, R.; Radimerski, T.; Raynaud, F. I.; Robertson, A.; Roughley, S. D.; Schoepfer, J.; Simmonite, H.; Sharp, S. Y.; Surgenor, A.; Valenti, M.; Walls, S.; Webb, P.; Wood, M.; Workman, P.; Wright, L. Combining hit identification strategies: fragment-based and in silico approaches to orally active 2-aminothieno[2,3-*d*]pyrimidine inhibitors of the Hsp90 molecular chaperone. *J. Med. Chem.* **2009**, *52*, 4794–4809.
- (45) Sharp, S. Y.; Boxall, K.; Rowlands, M.; Prodromou, C.; Roe, S. M.; Maloney, A.; Powers, M.; Clarke, P. A.; Box, G.; Sanderson, S.; Patterson, L.; Matthews, T. P.; Cheung, K. M.; Ball, K.; Hayes, A.; Raynaud, F.; Marais, R.; Pearl, L.; Eccles, S.; Aherne, W.; McDonald, E.; Workman, P. In vitro biological characterization of a novel, synthetic diaryl pyrazole resorcinol class of heat shock protein 90 inhibitors. *Cancer Res.* **2007**, *67*, 2206–2216.
- (46) Ohba, S.; Hirose, Y.; Yoshida, K.; Yazaki, T.; Kawase, T. Inhibition of 90-kD heat shock protein potentiates the cytotoxicity of chemotherapeutic agents in human glioma cells. *J. Neurosurg.* **2010**, *112*, 33–42.
- (47) Simoni, D.; Romagnoli, R.; Baruchello, R.; Rondanin, R.; Rizzi, M.; Pavani, M. G.; Alloatti, D.; Giannini, G.; Marcellini, M.; Riccioni, T.; Castorina, M.; Guglielmi, M. B.; Bucci, F.; Carminati, P.; Pisano, C. Novel combretastatin analogues endowed with antitumor activity. *J. Med. Chem.* **2006**, *49*, 3143–3152.
- (48) Giannini, G.; Cabri, W.; Simoni, D.; Baruchello, R.; Carminati, P.; Pisano, C. PCT Int. Appl. WO2010000748A1, 2010. Sigma-Tau Research Switzerland S.A. retains the property rights of all the compounds mentioned in the paper.
- (49) A preliminary metabolism study on human cryopreserved hepatocytes, performed on four representative compounds (**26**, **46**, **57**, **73**), revealed that this class of inhibitors possesses metabolic stability higher than the reference compound **10** (Table S2).
- (50) Kim, J.; Felts, S.; Llauger, L.; He, H.; Huezo, H.; Rosen, N.; Chiosis, G. Development of a fluorescence polarization assay for the molecular chaperone Hsp90. *J. Biomol. Screening* **2004**, *9*, 375–381.